

Phase behavior and free interfaces of a lattice-gas nematic-liquid-crystal model

Martin A. Bates

Department of Chemistry, University of Southampton, Southampton SO17 1BJ, United Kingdom

(Received 5 December 2001; published 2 April 2002)

The phase behavior of a mesogenic lattice-gas model consisting of molecules located at the sites of a three-dimensional cubic lattice has been studied using grand canonical Monte Carlo simulations. When two neighboring sites are occupied, the molecules interact via a potential composed of an isotropic lattice-gas (LG) term and an anisotropic Humphries-Luckhurst-Romano (HLR) term [Mol. Phys. **42**, 1205 (1981)]. The LGHLR model is shown to exhibit either nematic-isotropic, nematic-vapor (NV), and isotropic-vapor (IV) coexistence or just nematic-isotropic fluid coexistence, depending on the strength of the isotropic term. The liquid-vapor (i.e., NV and IV) interfaces were studied using canonical Monte Carlo simulations. By controlling the strength of the term that governs the anisotropy in the attractive forces, either planar or homeotropic anchoring is observed at the NV interface. The temperature dependencies of the density and order parameter profiles across the interfaces are determined for these two anchoring geometries.

DOI: 10.1103/PhysRevE.65.041706

PACS number(s): 64.70.Md, 64.70.Fx, 61.20.Ja

I. INTRODUCTION

Liquid crystals exhibit a rich interfacial behavior, including phenomena such as wetting and layering. Whilst these phenomena can also be observed in simple liquids, liquid crystals can exhibit additional interfacial phenomena due to their orientational degrees of freedom [1]. The least restricted symmetry breaking interface is that between a nematic liquid crystal and its saturated vapor and, even under these conditions, a range of different phenomena can occur. For example, the molecular orientation at the interface is not universal, but is found to be perpendicular, tilted, or parallel to the normal to the interface; these three anchoring geometries are known as planar, tilted, and homeotropic, respectively [1].

Early theoretical explanations of the nematic-vapor (NV) interface were based on phenomenological descriptions [2,3], but more recent molecular theories based on generalized van der Waals theory have been used to analyze the behavior of the liquid-crystal-vapor interface [4–7]. However, mapping of the expansion terms in these theories onto physical molecular interactions is not straightforward. To investigate how the experimental interfacial phenomena are related to the molecular potentials, a number of simulations of the free interface of nematic liquid crystals have, therefore, been performed [8–10]. These studies each concentrate on a single but different parametrization of the Gay-Berne potential [11], a liquid-crystal model that is extremely successful in reproducing bulk liquid-crystal behavior [12]. By combining the results of these simulations, Mills *et al.* [10] concluded that the preferred orientation at the free interface is determined by the ratio of the relative length of the molecule and the relative interaction energies for side-by-side and end-to-end configurations. This somewhat empirical view is backed up by naive arguments based on the relative energies of the cleavage planes for the different interface geometries for perfectly ordered close packed structures. However, the potential contains two further parameters (see Ref. [12]), and the influence of these parameters on the surface alignment should not be totally ignored. Fine tuning of the parametrization of Gay-Berne models to investigate NV interfaces, whilst possible, is clearly a difficult task since for each model the possibility of nematic-vapor coexistence must first be explored (which is not *a priori* obvious [13]), before simulations of the interface can be performed.

In this paper, we develop a simple lattice-based simulation model for the study of liquid-crystal-vapor interfaces. Such primitive models contain the basic physics of the system of interest, but have the detailed short range structure stripped away. This class of potentials is useful if we require an understanding of the truly generic or universal features of a system, that originate at longer length scales than the molecular size [14]. Their simplicity allows full phase diagrams for a particular model to be computed relatively quickly. In addition, it should also be possible to investigate systems containing interfaces of much larger dimensions than the more computationally demanding potentials, such as the Gay-Berne model, and, therefore, the lattice-based models readily lend themselves to the simulation of both confined and unconfined liquid crystals at the mesoscopic level. We do, of course, need to be sure that the simpler models can reproduce the realistic behavior exhibited by the more computationally demanding models.

The model is introduced in the following section. Grand canonical Monte Carlo simulations, used to determine the phase behavior, are discussed in Sec. III. Canonical ensemble simulations of the nematic-vapor and isotropic-vapor (IV) interfaces are described in Sec. IV and our conclusions are presented in Sec. V.

II. LATTICE-GAS HUMPHRIES-LUCKHURST-ROMANO MODEL

The lattice-gas model, which is isomorphic to the well-known Ising magnet model through a change of variables, is probably the most simple model with which to investigate liquid-vapor condensation phenomena [15,16]. Each lattice site can host either zero or one particle (atom, molecule) with the total occupation of the lattice, or density ρ , governed by an imposed chemical potential μ . The pair potential between two sites i and j is simply

$$U_{ij} = -s_i s_j \epsilon_{ij}, \quad (1)$$

where $s_i = 0, 1$ is the occupation number of site i and ϵ_{ij} is a positive constant ϵ for neighboring lattice sites and zero otherwise. This model exhibits liquid-vapor (or high-density–low-density) coexistence at low temperatures. As the temperature is increased, the density gap between the two phases decreases and eventually the coexistence curve is terminated by a critical point, as we expect for a typical liquid-gas coexistence curve [16].

A recent extension to this lattice-gas model to investigate nematic liquid crystals has recently been proposed [17] to take into account anisotropic interactions between the molecules by multiplying the lattice-gas interaction by the anisotropic term in the well-known Lebwohl-Lasher potential [18], resulting in a potential of the form

$$U_{ij} = -s_i s_j \epsilon_{ij} P_2(\cos \beta_{ij}). \quad (2)$$

Here $P_2(x)$ is the second rank Legendre polynomial $P_2(x) = \frac{1}{2}(3x^2 - 1)$, β_{ij} is the angle between the symmetry axes of molecules i and j , and the lattice has simple cubic geometry. This potential was found to exhibit nematic-isotropic (NI) coexistence, and the phase behavior was analyzed in terms of mixtures of rod-shaped and spherical molecules [17]. A reinterpretation of the phase behavior in terms of a single component system is also possible [19]. This reinterpretation points out a flaw of this model if we wish to simulate single component systems, in that it does not exhibit an isotropic liquid, rather just an isotropic fluid. The important distinction here is that the liquid can coexist with a distinct vapor phase, whilst the fluid has a continuous equation of state. In the limit of full lattice occupancy, this model is equivalent to the Lebwohl-Lasher model, which has been used extensively to investigate liquid crystals in both the bulk [20,21] and in confined geometries [21]. Of course, since the lattice occupation is always fixed (at $\rho = 1$), the density of the liquid crystalline material cannot change in such simulations and the only interfaces that can be studied are hard, in the sense that the density drops from $\rho = 1$ (liquid) to $\rho = 0$ (vapor) within one lattice spacing.

The introduction of a liquid-vapor coexistence curve into the phase diagram is straightforward [19]. If the potential contains an independent isotropic term in addition to the anisotropic term, this should provide the possibility for liquid-vapor coexistence for the following reason (see also Fig. 1). If no additional isotropic term is present in the model, the system exhibits only nematic and fluid phases [Fig. 1(a)]. The addition of an isotropic term should favor liquid-vapor coexistence ending in a critical point, as for the simple lattice-gas model [Eq. (1)]. However, if the isotropic term is weak, then the critical point for liquid-vapor coexistence, which would occur if no anisotropic term was present, will be located at low temperature, below the envelope of the nematic-isotropic fluid transition, and so this term will only reinforce the separation of the nematic and fluid phases. As the strength of the isotropic term is increased, we expect that the temperature at which the (metastable) IV critical point occurs will also increase, and so this will eventually occur at

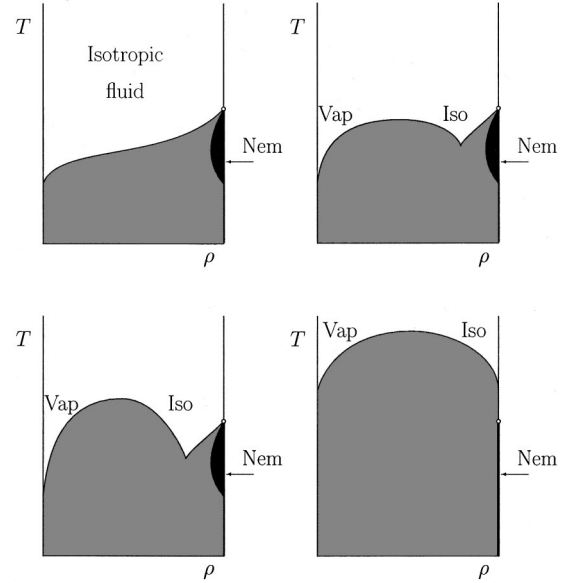


FIG. 1. Schematic phase diagrams (temperature vs density) for liquid crystal forming lattice-based models. The coexistence regions are shaded gray and the nematic regions black. (a) The anisotropic interaction dominates the pair potential between two molecules and if a liquid phase is formed, it will be nematic. If the anisotropic and isotropic interactions are balanced, then both isotropic and nematic liquids are observed, with the isotropic phase distinct from the (isotropic) vapor; the IV critical point may be below (b) or above (c) the temperature at which the nematic-isotropic transition occurs at full occupancy. (d) The isotropic term in the potential dominates, and the system phase separates into isotropic liquid and vapor phases well above the temperature at which the nematic-isotropic transition takes place in a fully occupied lattice. Note that a nematic phase is guaranteed even for the latter case, if the fully occupied lattice model exhibits a nematic phase, but in this situation it is confined to the isochore $\rho = 1$.

a temperature similar to the NI transition temperature at full lattice occupancy. This means that all three phases will be present in the phase diagram [Figs. 1(b) and 1(c)]. In the limit that the isotropic term overwhelms the anisotropic term, then we expect that the system will phase separate into a fully saturated lattice corresponding to an isotropic liquid and an unoccupied lattice corresponding to a vapor phase well above the NI transition temperature at full lattice occupancy. In this case, the nematic phase will be confined to the fully occupied lattice region, that is, $\rho = 1$ [see Fig. 1(d)]. Whilst this means that we can guarantee that the model will exhibit a nematic phase, we cannot be sure whether there will be an isotropic fluid phase or two distinct liquid and vapor phases.

Such observations were found to be the case for the lattice-gas Lebwohl-Lasher (LGLL) model [19], for which the interaction between the molecules is written as

$$U_{ij} = -s_i s_j \epsilon_{ij} [\lambda + P_2(\cos \beta_{ij})], \quad (3)$$

in which λ governs the strength of the additional isotropic term. As previously noted, a balance must be struck between the strength of the isotropic and anisotropic terms. If λ is too

weak, the model will behave as the original model [Eq. (2)]. In contrast, if λ is too strong, then the liquid-vapor coexistence curve will be present at temperatures that are relatively high, so that the liquid phase will correspond to a fully occupied lattice at temperatures of interest near the isotropic-nematic transition temperature and the nematic phase will be confined to the fully saturated lattice. The density profile at the corresponding NV interface would be expected to drop rapidly from $\rho=1$ to $\rho=0$ for all temperatures at which the nematic phase is stable. To determine the range of λ over which reasonable liquid-crystal behavior is exhibited for the LGLL model, grand canonical simulations were performed [19]. The model was found to exhibit either a two-phase phase diagram involving only nematic and isotropic fluid phases, or a three-phase phase diagram involving isotropic liquid and vapor phases in addition to the nematic phase [19] (see also Fig. 1).

Although the LGLL model shows the distinct condensed phases we wish to explore, there is a problem when it comes to investigate the interfacial behavior, in particular, the surface alignment. As the anisotropic potential depends only on the relative orientations of the pair of molecules, the model cannot distinguish between planar, tilted, and homeotropic anchoring at the NV interface. This is because all three geometries are equivalent in energy since they are related via a simple rotation of the molecular orientations, which preserves the angles between the molecules. Despite the fact that the Lebwohl-Lasher model has been extremely successful in reproducing the bulk behavior of nematic liquid crystals, it was recognized quite early on that it is unrealistic in its assumption that the interaction energy is independent of the orientation of the molecular vector [22], although it has since been used in the majority of lattice-based simulations of liquid crystals [21].

One way to overcome this problem for the lattice-gas models described here would be to add a phenomenological term to the potential, so that if one (or more) of the neighboring sites of molecule i was not occupied, the potential would depend on the angle between molecule i and the vector joining the occupied and unoccupied sites. However, a somewhat more appropriate approach is to use a model in which the anisotropic intermolecular forces are taken into account in a more rigorous way. Humphries, Luckhurst, and Romano (HLR) [22] developed such a lattice-based model by expanding the anisotropic pair potential for a pair of linear molecules, and relating the expansion coefficients to the anisotropy in the polarizability. The resulting potential has the form

$$U_{ij} = \gamma \epsilon_{ij} \left\{ 1 - \frac{3}{2} (\hat{u}_i \cdot \hat{r})^2 - \frac{3}{2} (\hat{u}_j \cdot \hat{r})^2 \right\} + \frac{3}{2} \gamma^2 \epsilon_{ij} \{ (\hat{u}_i \cdot \hat{r})^2 + (\hat{u}_j \cdot \hat{r})^2 - 9 (\hat{u}_i \cdot \hat{r})^2 (\hat{u}_j \cdot \hat{r})^2 + 6 (\hat{u}_i \cdot \hat{r}) (\hat{u}_j \cdot \hat{r}) (\hat{u}_i \cdot \hat{u}_j) - (\hat{u}_i \cdot \hat{u}_j)^2 \}, \quad (4)$$

where γ is the anisotropy in the polarizability of the molecule $(\alpha_{\parallel} - \alpha_{\perp}) / (\alpha_{\parallel} + 2\alpha_{\perp})$. As for the Lebwohl-Lasher model, ϵ_{ij} is equal to ϵ for nearest neighbors and zero

otherwise. The potential is expressed in terms of the unit vectors \hat{u}_i , \hat{u}_j , and \hat{r} that describe the orientations of molecules i and j and the intermolecular vector, respectively. In contrast to the Lebwohl-Lasher potential, the potential for parallel molecules is dependent on the orientation of the intermolecular vector; the potential energies corresponding to the side-by-side and end-to-end arrangements, for example, are $\gamma\epsilon - \frac{3}{2}\gamma^2\epsilon$ and $-2\gamma\epsilon - 3\gamma^2\epsilon$, respectively [22]. We should point out that, whilst it might be tempting to relate values of γ in the model to the components of the polarizability tensor α for real molecules, this is probably not an effective route of determining that values of γ will lead to interesting phase behavior. This is because the anisotropy in the polarizability does not dominate the interaction between real molecules, and important terms such as the shape of the molecule and electrostatic interactions are neglected in the HLR lattice model. Thus γ should be viewed only as an effective parameter that governs the total anisotropy in the molecular interactions, not just those interactions arising from the anisotropy in the polarizability.

It is appropriate to point out that whilst the authors of Ref. [22] performed simulations for a number of values of γ for the fully saturated cubic lattice, this was not actually necessary. Although γ appears to be a variable parameter in the HLR model [see Eq. (4)], it turns out not to be for the case of a fully saturated lattice. This statement is easy to understand when we consider that the term linear in γ involves an expression of the form $\Sigma (\hat{u}_i \cdot \hat{r})^2$, in which, for the cubic lattice, \hat{r} is summed over the x , y , and z axes (and the $-x$, $-y$, and $-z$ axes). This term is nothing other than the sum of the direction cosines squared for the vector describing the orientation of the molecule and so is not dependent on the molecular orientation. This means that the linear term in γ is simply a scalar that only shifts the total energy and so does not influence the phase behavior as the molecules in all possible phases have exactly the same number of neighbors since the lattice is fully occupied. Indeed, this is borne out by the fact that the data of Ref. [22] fall on the same curve for different values of γ . The only dependence of the phase behavior on γ is that this acts as a scaling variable for the temperature (i.e., $T^* = kT/\epsilon\gamma^2$). However, as we shall see, this is not the case for the lattice-gas models in which we are interested here, since the lattice is not fully occupied, and so the sums of type $\Sigma (\hat{u}_i \cdot \hat{r})^2$ are not over all six neighbors.

As we have already seen for the lattice-gas Lebwohl-Lasher model [Eq. (3)], the most interesting (and realistic) phase behavior was observed when there was a balance between the isotropic and anisotropic terms in the potential. We, therefore, define the lattice-gas Humphries-Luckhurst-Romano (LGHLR) potential as [compare Eqs. (2)–(4)]

$$U_{ij} = s_i s_j \epsilon_{ij} \left(-\lambda + \gamma \left\{ 1 - \frac{3}{2} (\hat{u}_i \cdot \hat{r})^2 - \frac{3}{2} (\hat{u}_j \cdot \hat{r})^2 \right\} + \frac{3}{2} \gamma^2 \{ (\hat{u}_i \cdot \hat{r})^2 + (\hat{u}_j \cdot \hat{r})^2 - 9 (\hat{u}_i \cdot \hat{r})^2 (\hat{u}_j \cdot \hat{r})^2 + 6 (\hat{u}_i \cdot \hat{r}) \times (\hat{u}_j \cdot \hat{r}) (\hat{u}_i \cdot \hat{u}_j) - (\hat{u}_i \cdot \hat{u}_j)^2 \} \right), \quad (5)$$

in which λ , the strength of the isotropic term, can be varied

to vary the phase behavior. Of course, for a fully occupied lattice, this potential has exactly the same phase behavior as the HLR model, since the additional scalar λ serves only to shift the total energy of the system equally in all phases. The addition of the lattice-gas term should lead to the possibility of investigating liquids in coexistence with their vapor phase and the HLR term guarantees us that a nematic phase will be observed, although as for the LGLL model [19], this may be restricted to the fully occupied lattice.

III. GRAND CANONICAL SIMULATIONS AND PHASE DIAGRAMS

The phase behavior of the different models was determined using grand canonical Monte Carlo simulations, in which the density of the system is not fixed but governed by the imposed chemical potential μ . The simulations were performed in the exactly same way as in the previous study of the LGLL model and full details are given in Ref. [19]. For each model studied, lattices of size 40^3 were used to determine the equations of state over a range of temperatures, from which the coexistence densities of the observed phases were extracted [19].

We start our discussion of the phase behavior by concentrating on models with $\gamma = -\frac{1}{2}$. For this value, the energy minimum occurs for pairs of molecules in a side-by-side arrangement. The phase diagrams for three different values of λ are shown in Fig. 2. For low values of λ [$\lambda = 0.00$ in Fig. 2(a)], a single first order transition is observed, between orientationally ordered and disordered phases. This is equivalent to the nematic-isotropic transition observed for the LGLL model with $\lambda = 0$ [17,19]. At low temperature, an artifact of the model occurs in which planes of highly ordered molecules are observed, every other lattice spacing, at density $\rho = 0.5$. These are observed because, for $\gamma = -\frac{1}{2}$, the relative energies for a pair of molecules in the side-by-side and end-to-end configurations are $-\frac{7}{8}\epsilon$ and $+\frac{1}{4}\epsilon$. Since the energy of the end-to-end configuration is greater than zero, that is, above the energy of interaction of a molecule with an empty site, it is energetically more favorable to microphase separate at intermediate densities ($\rho \sim 0.5$) into planes of orientationally ordered side-by-side molecules, each separated by an empty plane. This artifact disappears when $\lambda > 0.25$, that is, when the interaction energy for end-to-end pairs is lower than that than for a molecule interacting with an empty site, the situation we expect for real molecules. However, this value of λ is well below the range for which interesting phase behavior occurs.

On increasing λ , an isotropic liquid-vapor transition terminated by a critical point is induced [$\lambda = 1.75$ in Fig. 2(b)] and as λ is increased further, the envelope of the isotropic-vapor transition is shifted to higher temperatures, whilst the location of the nematic-isotropic coexistence region is essentially unaffected [$\lambda = 2.00$ in Fig. 2(b)]. This behavior is entirely as we expect for the following region. Since the energy parameter for the isotropic lattice-gas model [Eq. (1)] simply scales the temperature dependence of the coexistence curve and, therefore, the critical point for liquid-vapor separation,

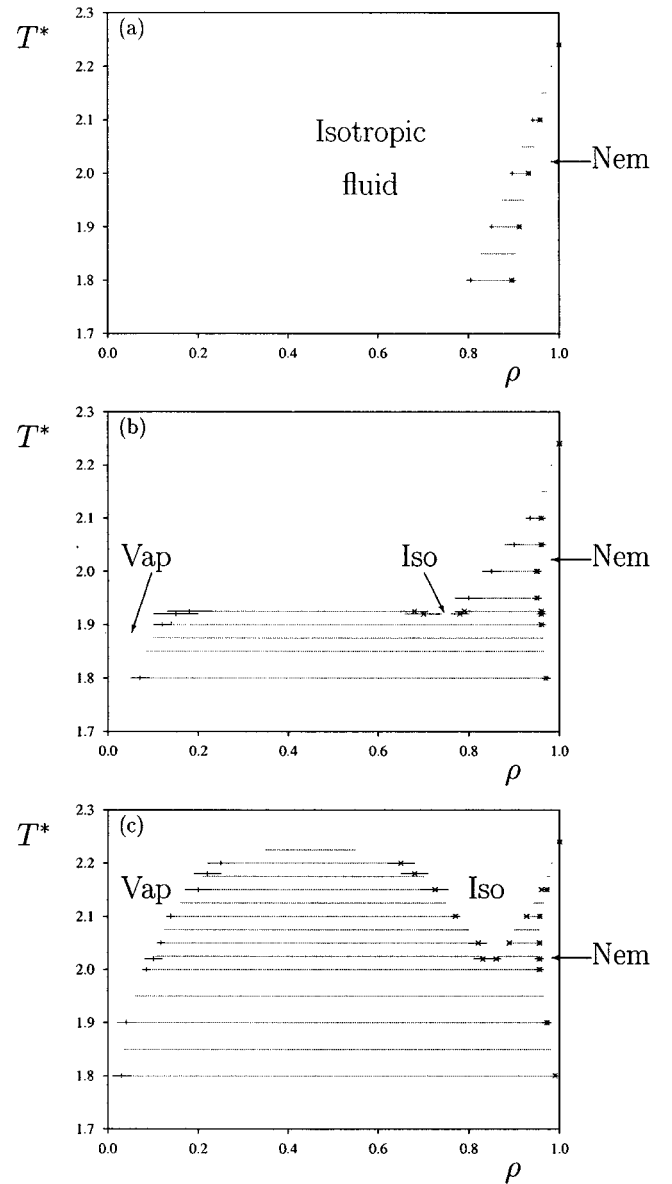


FIG. 2. Phase diagrams for the lattice-gas Humphries-Luckhurst-Romano model with $\gamma = -\frac{1}{2}$. (a) $\lambda = 0$, isotropic- (fluid) nematic phases. For (b) $\lambda = 1.75$ and (c) $\lambda = 2.00$, distinct isotropic liquid and vapor phases are observed. Units: $T^* = kT/\epsilon\gamma^2$. The lines indicate the coexistence regions.

we expect that an increase in the isotropic contribution λ to the anisotropic potential will scale the coexistence curve to higher temperatures. If the anisotropic terms were not present in the potential, an increase in λ is of course equivalent either increasing ϵ in Eq. (1) at constant temperature or, conversely, lowering the temperature ($T^* = kT/\epsilon$) at fixed ϵ , which leads to a widening of the density gap between the liquid and vapor phases. Moreover, we do not expect the location of the nematic-isotropic coexistence region to shift dramatically since, at least at the higher temperatures in which we are interested in, this transition occurs between two relatively dense phases, of similar density. Thus the addition of the scalar term λ to the potential will to a first

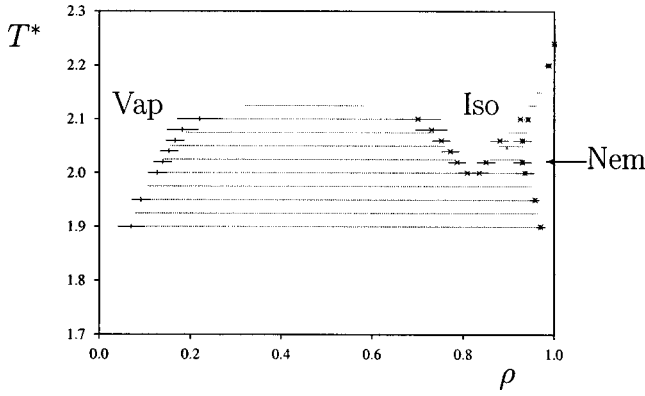


FIG. 3. Phase diagram for the lattice-gas Humphries-Luckhurst-Romano model with $\gamma = +\frac{1}{2}$, and $\lambda = 2.00$. Units as in Fig. 2. The lines indicate the coexistence regions.

approximation influence the energy of both phases equally, and so will not shift the phase boundaries.

A similar series of phase diagrams are observed for $\gamma = +\frac{1}{2}$, and a typical phase diagram for the model with $\lambda = 2.0$ is shown in Fig. 3. Note that an artifact similar to the one observed for negative γ also occurs at low temperature for positive γ when the isotropic contribution to the potential is weak (i.e., $\lambda \sim 0.0$); here, strings of highly ordered molecules are observed, since the energy of a pair of molecules in the side-by-side arrangement is greater than zero. As before, this artifact disappears when the energy for a pair of interacting molecules is lower than zero, that is, when $\lambda > \frac{1}{8}$.

IV. LIQUID-VAPOR INTERFACES

To study the interfaces, canonical Monte Carlo simulations were performed in an elongated box of size $40 \times 40 \times 80$ containing 64 000 molecules (corresponding to 50% occupation), with full periodic boundary conditions. The initial configuration for each model was taken to be a dense slab in the middle of the box, which was heated to a temperature corresponding to a stable liquid phase, below the critical point. The system was then cooled through the isotropic and nematic phases to investigate the interfaces, and then reheated to check for any hysteresis effects. Heating the system lead to essentially the same profiles at each state point, and so we will discuss only those obtained from the cooling runs.

The variation of the density through the interface can be monitored by the density profile, $\rho(z)$, from which the densities of the coexisting vapor and liquid phases, ρ_v and ρ_l , can be determined by fitting the simulation results to a hyperbolic tangent. Since two interfaces are present in the simulation box, the density profile was fitted to a double hyperbolic tangent of the form

$$\rho(z) = \rho_v + \frac{1}{2}(\rho_l - \rho_v) \left[\tanh\left(\frac{z - z_1}{2\delta}\right) - \tanh\left(\frac{z - z_2}{2\delta}\right) \right], \quad (6)$$

in which δ is the interfacial thickness and z_i is the location of the Gibbs dividing surface for interface i ($i = 1, 2$). The assumption that the interfacial thickness δ is equal for both interfaces is justified since the interfaces are equivalent, and on average just mirror images of each other. We note that, in principle, it would be possible to obtain the phase diagram determined in Sec. III from the fits of density profiles and this method would require only one simulation for each temperature for which two-phase coexistence is observed and two simulations for the case of three phases. As it is relatively easy to choose an average density in the middle of the isotropic-vapor coexistence curve, obtaining this part of the phase diagram would be straightforward, at least at temperatures away from the critical point. However, since the grand canonical simulations are relatively cheap for low density systems, because overlap tests for lattice models are trivial, the grand canonical route is probably just as efficient. Moreover, to obtain coexistence densities from the interface system, we should ensure that the same results are obtained starting from lower temperatures and higher temperatures. In the latter case, this would mean waiting for the liquid slab to nucleate and then grow to form a uniform slab within the periodic boundaries. Preliminary simulations indicated that this process may be slow as sometimes two or more liquid regions form and only slowly coalesce to form a single liquid region. Estimating a reasonable value for the density in the middle of the nematic-isotropic coexistence region is not so straightforward as for the liquid-vapor case since this is rather narrow, if indeed it exists, which we do not know *a priori*. Thus it is more appropriate to use the grand canonical route to the equations of state and, therefore, to the coexistence densities.

The orientational order of the molecules through the box was characterized by the following profiles:

$$\sigma(z) = \langle P_2(\hat{u}_i \cdot \hat{n}(z)) \rangle_{(z)}, \quad (7)$$

$$\eta(z) = \langle P_2(\hat{u}_i \cdot \hat{z}) \rangle_{(z)}, \quad (8)$$

where $\langle \dots \rangle_{(z)}$ implies the average of the function, determined at z , \hat{z} is a unit vector along the z axis and $\hat{n}(z)$ is defined as the director within the thin slab at position z . The former profile indicates the extent of the orientational order across the interface, irrespective of the average direction of alignment. The latter profile contains information on the average alignment direction. For perfect order parallel to the interfacial normal, $\eta = 1$, and for perfect order perpendicular to the interfacial normal, $\eta = -\frac{1}{2}$. Other definitions of interfacial order parameters commonly determined for liquid crystalline interfaces are possible [4–10, 23, 24].

Before we discuss the results, it is worth noting that we can use energetic arguments similar to those invoked by Mills *et al.* [10] when considering Gay-Berne interfaces. The potential energies for a pair of molecules in the side-by-side and end-to-end arrangements are, as noted in Sec. II, $\gamma\epsilon - \frac{3}{2}\gamma^2\epsilon$ and $-2\gamma\epsilon - 3\gamma^2\epsilon$, respectively [22]. Therefore, if we consider the limiting case of a perfectly ordered nematic

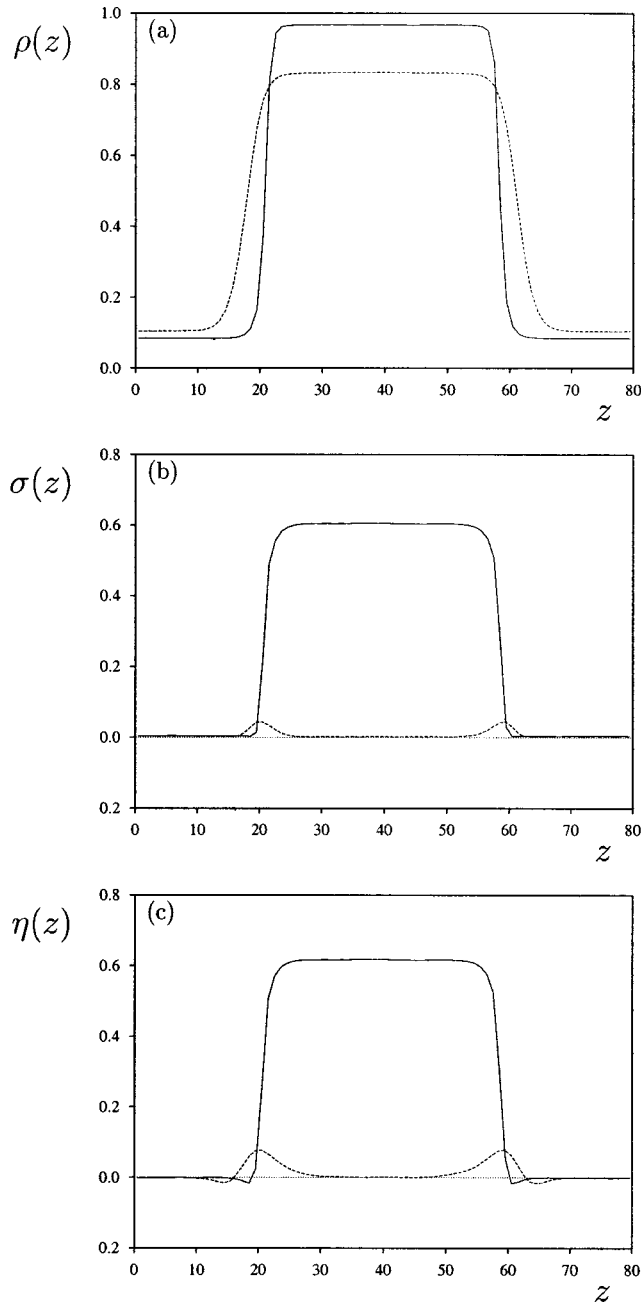


FIG. 4. Interfacial profiles (a) $\rho(z)$, (b) $\sigma(z)$, (c) $\eta(z)$ for the LGHLR model $\gamma = -\frac{1}{2}$, $\lambda = 2.00$ at temperatures $T^* = 2.00$ (solid line) and 2.01 (dashed line), corresponding to nematic-vapor and isotropic-vapor coexisting systems, respectively.

region, at density $\rho = 1$, the surface free energy will be proportional to $\frac{3}{2}\gamma^2\epsilon - \gamma\epsilon$ for planar alignment at the surface and $2\gamma\epsilon + 3\gamma^2\epsilon$ for homeotropic alignment. For γ negative, the lower surface energy corresponds to homeotropic alignment; in contrast, following this argument for γ positive we expect to observe planar alignment at the interface.

The density and order parameter profiles are shown in Fig. 4 for the case of $\gamma = -\frac{1}{2}$ and $\lambda = 2$, at temperatures just above and just below the triple point. For the lower temperature shown, the liquid phase is nematic, as indicated by the finite value of σ in the center of the dense region. Moreover,

since $\eta(z) = \sigma(z)$ in this region, the director must be aligned along the z axis, and, therefore, we may conclude that the molecules at the interface align in a homeotropic arrangement, and that this orientational order propagates into the bulk. Similar profiles are observed for lower temperatures, with the difference in coexistence densities gradually becoming larger and the order parameters for the nematic region increasing with decreasing temperature. At the higher temperature shown in Fig. 4, the liquid phase is isotropic, as indicated by the vanishing value of $\sigma(z)$ and $\eta(z)$ in the center of the denser region. However, we observe that the profiles for both $\sigma(z)$ and $\eta(z)$ are finite and positive in the region corresponding to the liquid side of the interface. This indicates that, even though the bulk phase is isotropic, the free surface influences the alignment within a narrow region near the surface, with the molecules tending to align parallel to the interfacial normal. Such enhanced surface order has been observed for the isotropic phase of Gay-Berne systems [8–10]. Note also that the profile $\eta(z)$ changes from positive on the isotropic side of the interface to negative on the vapor side. This was observed also for Gay-Berne systems [8] and for other uniaxial molecular potentials, such as the dumbbell model for chlorine [25]; Sluckin has given a qualitative explanation of this phenomenon [26]. Similar profiles are observed for all higher temperatures, with the difference in coexisting densities decreasing as the temperature is increased and the excess order at the surface gradually disappearing. As the temperature is increased above the critical point, the interfaces are, of course, found to disappear as there is no distinction between a vapor and a liquid.

The equivalent profiles are shown in Fig. 5 for the model with parameters $\gamma = +\frac{1}{2}$ and $\lambda = 2$, at temperatures either side of the triple point. The density profiles are essentially equivalent to those for the previous model with homeotropic alignment at the surface. The finite value of the profile $\sigma(z)$ in the center of the dense phase clearly indicates that the lower temperature corresponds to a nematic-vapor interface. The negative value of $\eta(z)$ in the same region indicates that the average direction of alignment is perpendicular to the z axis, that is, there is planar alignment at the interface that propagates through the nematic liquid region. Note that the orientational order parameter profile $\sigma(z)$ has a different form to that observed for the previous model in the vicinity of the isotropic-vapor interface. For the homeotropic system, this was observed to go through a maximum at the interface; here, the profile is flat across the interface. In contrast, the profile for $\eta(z)$ is nonzero and negative, essentially an inverted version to the one observed for the homeotropic model. Thus we may conclude that the molecules in the vicinity of the surface of the isotropic region align perpendicular to the interfacial normal, that is, in a planar arrangement. This also explains the fact that the profile $\sigma(z)$ is zero across the interface. Since the molecules align, on average, perpendicular to the surface normal, they are still free to adopt any orientation in plane and so this results in an order parameter of zero. This contrasts the case of homeotropic alignment, when the molecules align parallel to the surface normal, and so there is less rotational freedom leading to a finite value for $\sigma(z)$.

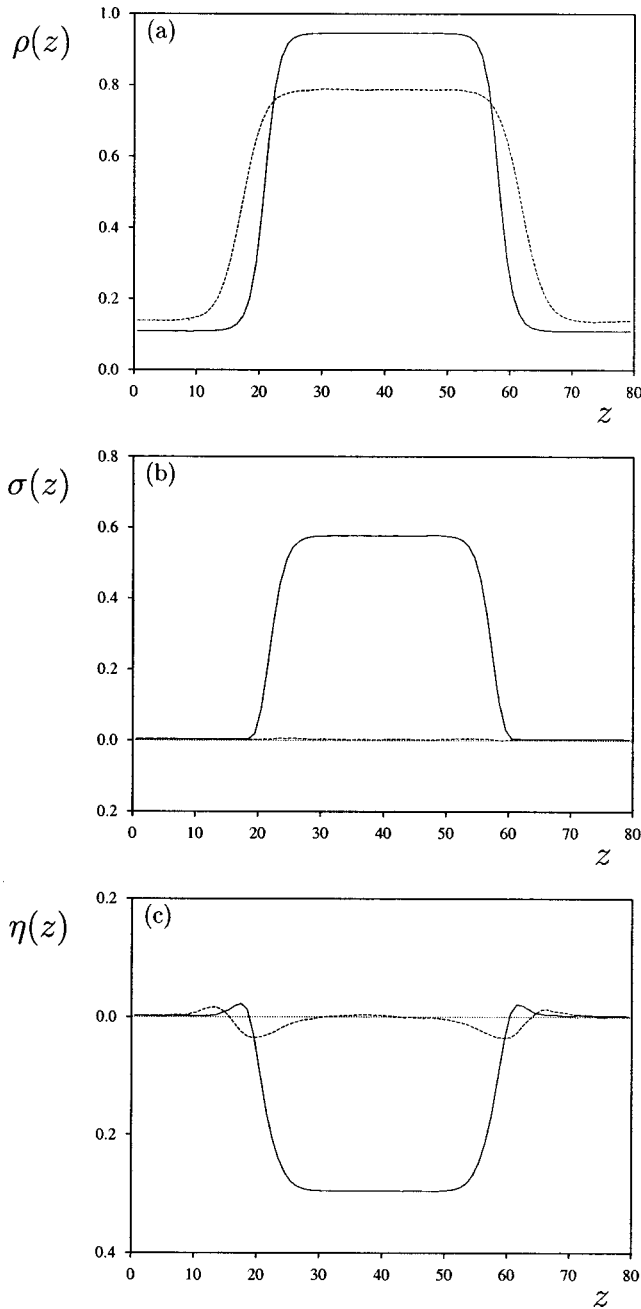


FIG. 5. Interfacial profiles (a) $\rho(z)$, (b) $\sigma(z)$, (c) $\eta(z)$ for the LGHLR model $\gamma = +\frac{1}{2}$, $\lambda = 2.00$ at temperatures $T^* = 1.99$ (solid line) and 2.00 (dashed line), corresponding to nematic-vapor and isotropic-vapor coexisting systems, respectively.

V. CONCLUSIONS

We have introduced a lattice-based model with which to study the phase behavior and interfaces of nematic liquid crystals. Whilst using a lattice-based system means that the chemical detail has been lost, in comparison to atomic detailed and the more generic Gay-Berne systems, the use of a lattice model has a clear advantage in that much larger systems can be studied over a large range of state points, relatively quickly. The use of such coarse grained, but still molecular based, potentials will be important if we wish to

investigate phenomena at the mesoscale level using simulation. The model introduced here also has the advantage over other lattice models in that it is a lattice-gas type model, rather than a fully occupied lattice model. This means that the density of the system is allowed to change and so this class of potential can be used to investigate phase transition at which a density change occurs, and so can also be used to study interfaces between phases of intermediate density, that is not just hard interfaces of the type $\rho = 0$ to $\rho = 1$.

Whilst the model is relatively simple in form, it has been shown to exhibit the interfacial phenomena that have been observed in simulations of Gay-Berne systems, such as the surface enhanced ordering at the isotropic surface, the change in sign of the order parameter $\eta(z)$ at the interface, and either homeotropic or planar ordering at the surface. The fact that the lattice-based model can reproduce the behavior exhibited by the more computational demanding molecular potentials gives us confidence that, despite its simplicity, it should provide a useful model with which to study liquid-crystal interfaces, especially at larger length scales than those available in simulations of Gay-Berne systems. In addition, using energetic arguments, similar to those used by Mills *et al.* [10] to try to explain the interfacial alignment of Gay-Berne systems, we can speculate that models with a negative γ will lead to a homeotropic surface alignment, whereas planar alignment will be observed for γ positive. It is, therefore, relatively straightforward to choose a model that will lead to certain required anchoring conditions at the free interface. We have not modified the magnitude of the parameter γ , rather just studied a single positive and negative value. This is clearly a parameter that could be modified to vary the behavior of the mesogen; for example, the magnitudes of the order parameter profiles may change in the vicinity the surface. However, it seems unlikely that changing the magnitude of γ will change the actual alignment at the surface due to simple energetic arguments.

Finally, it is worth pointing out that, although the model has been described as a one component system, it can also be thought of as a two component system of rods (R) and spheres (S) (see also Ref. [17]). In this case, the interactions between the particles are

$$U_{S-S} = \epsilon^*,$$

$$U_{R-S} = \epsilon^*,$$

$$U_{R-R} = \epsilon^* + U_{\text{LGHLR}}, \quad (9)$$

where the interaction energy ϵ^* between two spheres is the same as that between a rod and a sphere, and this isotropic interaction is added to the interaction between two rods. In this case, the imposed chemical potential would actually be the chemical potential difference between the rods and spheres [27]; this would of course lead to exactly the same phase diagrams as those determined here for the single

component system, since here the imposed chemical potential is simply the chemical potential of a rod with respect to that of an empty site. The only difference between the one and two component systems would be the shift in the total potential energy.

ACKNOWLEDGMENTS

M.A.B wishes to thank the Royal Society for the award of a grant for the Linux PC cluster on which these simulations were run.

-
- [1] T. J. Sluckin and A. Poniewierski, in *Fluid Interfacial Phenomena*, edited by C. Croxton (Wiley, New York, 1986).
- [2] P. Sheng, *Phys. Rev. A* **26**, 1610 (1982).
- [3] A. Poniewierski and T. J. Sluckin, *Liq. Cryst.* **2**, 281 (1987).
- [4] M. M. Telo da Gama, in *Observation, Prediction and Simulation of Phase Transitions in Complex Fluids*, edited by M. Baus, L. F. Rull, and J.-P. Ryckaert (Kluwer Academic, Dordrecht, 1995).
- [5] E. Martin del Rio, M. M. Telo de Gama, E. de Miguel, and L. F. Rull, *Phys. Rev. E* **52**, 5028 (1995).
- [6] E. Martin del Rio, M. M. Telo da Gama, E. de Miguel, and L. F. Rull, *Europhys. Lett.* **35**, 189 (1996).
- [7] F. N. Braun, T. J. Sluckin, E. Velasco, and L. Mederos, *Phys. Rev. E* **53**, 706 (1996).
- [8] E. Martin del Rio and E. de Miguel, *Phys. Rev. E* **55**, 2916 (1997).
- [9] A. P. J. Emerson, S. Faetti, and C. Zannoni, *Chem. Phys. Lett.* **271**, 241 (1997).
- [10] S. J. Mills, C. M. Care, M. P. Neal, and D. J. Cleaver, *Phys. Rev. E* **58**, 3284 (1998).
- [11] J. G. Gay and B. J. Berne, *J. Chem. Phys.* **74**, 3316 (1981).
- [12] M. A. Bates and G. R. Luckhurst, *Struct. Bonding (Berlin)* **94**, 65 (1998).
- [13] E. de Miguel, E. M. del Rio, J. T. Brown, and M. P. Allen, *J. Chem. Phys.* **105**, 4234 (1996).
- [14] K. A. Dawson, in *Computer Simulation in Chemical Physics*, edited by M. P. Allen and D. J. Tildesley (Kluwer Academic, Dordrecht, 1993).
- [15] D. A. Chesnut and Z. W. Salsburg, *J. Chem. Phys.* **38**, 2861 (1963).
- [16] D. Chandler, *Introduction to Modern Statistical Mechanics* (Oxford University, Oxford, 1987), Chap. 5.
- [17] M. A. Bates, N. Halim, R. Hashim, G. R. Luckhurst, S. Romano, and S. M. Zain (unpublished).
- [18] P. A. Lebowl and G. Lasher, *Phys. Rev. A* **6**, 426 (1972).
- [19] M. A. Bates, *Phys. Rev. E* **64**, 051702 (2001).
- [20] U. Fabbri and C. Zannoni, *Mol. Phys.* **58**, 763 (1986).
- [21] P. Pasini, C. Chiccoli, and C. Zannoni, in *Advances in the Computer Simulations of Liquid Crystals*, edited by P. Pasini and C. Zannoni (Kluwer Academic, Dordrecht, 2000).
- [22] R. L. Humphries, G. R. Luckhurst, and S. Romano, *Mol. Phys.* **42**, 1205 (1981).
- [23] M. A. Bates and C. Zannoni, *Chem. Phys. Lett.* **280**, 40 (1997).
- [24] M. A. Bates, *Chem. Phys. Lett.* **288**, 209 (1998).
- [25] S. M. Thomson and K. E. Gubbins, *J. Chem. Phys.* **70**, 4947 (1979).
- [26] T. J. Sluckin, *Mol. Phys.* **43**, 817 (1981).
- [27] D. Frenkel and B. Smit, *Understanding Molecular Simulations from Algorithms to Applications* (Academic, New York, 1996).